In-silico Evaluation of Bioactive Compounds from Medicinal Plants as Promising Inhibitory Agents against Mycobacterium tuberculosis dihydrofolate reductase

Olatunji K Toyosi[1*], Oladosu O. Peters[2], Kolawole O. Matthew[3]

[1,2]Department of Microbiology and Biotechnology, National Institute for Pharmaceutical Research and Development, Abuja, PMB 21, Federal Capital Territory, Nigeria.

[3]Infectious Disease and Environmental Health Research Group, Department of Microbiology, Faculty of Life Sciences, University of Ilorin, Ilorin, PMB 1515, Kwara State, Nigeria.

[*]Correspondence author

DOI: https://doi.org/10.51584/IJRIAS.2025.10030060

Received: 09 March 2025; Accepted: 13 March 2025; Published: 19 April 2025

ABSTRACT

Tuberculosis (TB) is one of the major public health challenges around the globe. Targeting dihydrofolate reductase (DHFR), a key enzyme involved in folate metabolism, is a promising path to discovering an effective TB treatment. This study assessed the molecular docking of eight bioactive compounds from two medicinal plants (Berlinia grandiflora and Senna occidentalis) to the active site of Mycobacterium tuberculosis dihydrofolate reductase (MtbDHFR) (6VVB.pdb). Molecular docking and computational tools were used to evaluate the binding energies and interactions with MtbDHFR active site. The chemical structures of the bioactive compounds and the 3D structure of the target protein were retrieved from the PubChem database and Research Collaboratory for Structural Bioinformatics (RCSB) Protein Data Bank, respectively. The binding energy of the bioactive compounds ranged between -4.468 to -6.146 kcal/mol, while the reference drug exhibited a binding energy of -5.392 kcal/mol. Interestingly, five compounds (4 to 8) showed stronger binding energies (-5.485 to -6.146 kcal/mol) than the reference drug, depicting them as promising antituberculosis agents. Among them, L-(+)-ascorbic acid 2, 6-dihexadecanoate exhibited the highest binding energy of -6.146 kcal/mol. Additionally, the compounds exhibited hydrogen bonds and hydrophobic interactions with the active site residues of the protein. Overall, the results indicate that these bioactive compounds exhibited favorable docking interactions with the target protein, highlighting their potential as therapeutic agents for TB drug discovery.

Keywords: Tuberculosis, molecular docking, medicinal plants, therapeutic drug

INTRODUCTION

Among infectious diseases, tuberculosis (TB) is one of the leading causes of death worldwide. The World Health Organization (WHO) declared TB a global health emergency in 1993 [1]. In Nigeria, it was also declared a national emergency in 2006, leading to the development of an emergency plan for TB control. Globally, an estimated 10.6 million people fell ill with TB in 2022, up from 10.3 million in 2021, with the majority of cases occurring in low- and middle-income countries, particularly in nations such as Nigeria, Pakistan, the Philippines, Bangladesh, China, India, Indonesia, and South Africa [2]. Geographically, in 2022, most TB cases were recorded in the WHO Regions of South-East Asia (46%), Africa (23%), and the Western Pacific (18%), with smaller proportions in the Eastern Mediterranean (8.1%), the Americas (3.1%), and Europe (2.2%). The total number of TB-related deaths, including those among people with HIV, was 1.3 million in 2022, down from 1.4 million in 2021. However, during the 2020-2022 period, COVID-19 disruptions led to nearly half a million additional TB-related deaths [2]. TB remains the leading cause of death among people with HIV due to the reciprocal relationship between these infections [3].

The development of TB depends on various factors, including the latency period of infection, the patient's age, and immunity [4]. Anti-TB treatments require long-term administration and are associated with several side effects, leading to treatment abandonment, which in turn facilitates the selection of multidrug-resistant mycobacterial strains [5]. Given the challenges related to treatment adherence, the growing spread of the etiological agent, and the emergence of multidrug-resistant (MDR-TB), extensively drug-resistant (XDR-TB), and totally drug-resistant TB (TDR-TB) strains, it is crucial to explore new strategies for TB control, including the development of new anti-TB medications [6]. The emergence of these resistant strains has been linked to the inappropriate use of TB medications, including incorrect prescriptions, substandard drug quality, and premature treatment discontinuation [2]. These drug-resistant strains show resistance to anti-TB drugs such as Ethionamide, Isoniazid, Ethambutol, Rifampicin, and Pyrazinamide [7].

The combination of advanced in-silico techniques and data from the three-dimensional structures of human and MtbDHFR has significantly advanced the search for novel TB drugs [8]. One of the validated drug targets for treating M. tuberculosis infection is dihydrofolate reductase (DHFR). DHFR is a crucial enzyme involved in the production of tetrahydrofolate (THF), which plays a key role in various cellular functions [9]. Specifically, DHFR converts dihydrofolate to tetrahydrofolate, contributing to thymidylate biosynthesis, DNA replication, RNA transcription, protein synthesis, and cell proliferation [10]. MtbDHFR, an NADPH-dependent enzyme in folate metabolism, is essential for mycobacterial growth [11]. MtbDHFR catalyzes the reduction of dihydrofolic acid (DHF) to tetrahydrofolic acid (THF) through hydride transfer, a reaction essential for metabolic pathways crucial for cell maintenance. MtbDHFR consists of 159 amino acid residues, with a secondary structure comprising a central β-sheet flanked by four α-helices [8]. THF is vital for the de novo biosynthesis of purines, thymines, and various amino acids. DHFR is a well-established target for treating various diseases, and inhibitors of this enzyme have been used as antibacterial, antifungal, antimalarial, and anticancer agents [9, 12]. Blocking the folate pathway in M. tuberculosis has been shown to result in bacterial cell death [13, 8]. Targeting the MtDHFR, is therefore a novel way to combat TB and can lead to new therapeutic treatments for TB patients.

Despite challenges such as drug resistance and adverse effects associated with existing TB treatments, there is growing interest in exploring natural products, particularly medicinal plants, as potential sources of new anti-TB agents. This highlights the urgent need for rapid drug development and continuous research efforts. Novel, potent, and safer anti-TB drugs are required to counter acquired resistance and shorten lengthy treatment regimens. Medicinal plants offer a diverse array of bioactive compounds with therapeutic potential [14]. Numerous bioactive compounds have been identified in plant extracts, leading to extensive drug discovery efforts focused on plants traditionally used to treat infections [15]. Medicinal plants remain a primary source of new compounds for developing innovative therapeutic drugs against various diseases [16]. Due to the adverse effects associated with anti-TB medications, many TB patients have turned to medicinal plants for treatment [17, 18]. These plants have been reported to contain numerous bioactive compounds with antimycobacterial activity [19]. The use of herbal and alternative therapies for TB treatment is increasing [20].

Senna occidentalis (L.) Link, also known as Coffee Senna, Negro Coffee, Coffee Weed, and Stinking Weed, is a member of the Fabaceae family and is found in various regions of Asia, Africa, and America. The plant often invades pastures, orchards, roadsides, and cultivated fields, particularly in soybean-growing areas [21, 22]. In Nigeria, especially in the northern region, S. occidentalis has been traditionally used as both food and medicine. The seeds of this plant are used as a diuretic and tonic, while its extracts are employed to treat pneumonia and TB, as well as to expel worms and relieve menstrual cramps [23]. Various parts of the plant exhibit anti-inflammatory, antioxidant, immunosuppressive, antihepatotoxic, antibacterial, antifungal, and antiplasmodial properties, making it a promising candidate for treating and controlling diseases. S. occidentalis possesses diuretic, purgative, expectorant, tonic, and febrifuge properties, making it useful in treating rheumatism, leprosy, sore eyes, typhoid, hematuria, hemoglobin disorders, and asthma [24]. Additionally, the plant has been found to aid in treating coughs and seizures, lowering blood pressure, and reducing spasms. Phytochemical analysis has identified bioactive compounds such as flavonoids, saponins, anthraquinones, alkaloids, tannins, terpenes, and glycosides in its extracts [25]. Research on its leaves and fruits has shown that it is a significant source of anthraquinones and flavonoids, with anti-inflammatory properties, muscle relaxation effects, and lipid peroxidation inhibition [22, 26]. These findings underscore the therapeutic potential of S. occidentalis in traditional medicine [24].

ISSN No. 2454-6194 | DOI: 10.51584/IJRIAS |Volume X Issue III March 2025

Berlina grandiflora (Vahl) Hutch. and Dalziel, a member of the Leguminasae family, is a widely used plant in Nigerian traditional medicine that is commonly found across West, South, and Central Africa. The Berlinia genus consists of approximately 20 species distributed across African countries such as Mali, Guinea, Nigeria, Central Africa Republic, Democratic Republic of Congo, and Ghana [27, 28]. In Nigeria, the Yoruba ethnic group refers to B. grandiflora as "Apado", while the Igbo ethnic group calls it "Ububa". The plant varies in form, ranging from a shrub of 2–5 m in height to a spreading tree with a dense, rounded crown reaching 20–30 m [29]. *B. grandiflora* is a complex acidic polysaccharide that is non-toxic, hydrophilic, biocompatible, and biodegradable [30]. The various components of the plant are used in numerous ethnomedicinal ways. The stem bark is used for treating gastrointestinal disorder and alleviate labor pain during childbirth. The bark infusion is used as laxative, the bark sap is used for healing sores and wounds, while bark decoctions are administered for hemorrhoids and liver ailments. Additionally, a decoction made from the leafy twigs is valued for its febrifuge, purgative, antiemetic, cholagogue properties, and also consumed as a tonic [31, 32, 33]. Research indicates that the leaves and stem bark of B. grandiflora exhibit antibacterial activity against Staphylococcus aureus, Escherichia coli, Alcaligenes faecalis, Serratia marcescens, Enterobacter bacteraerogenes, Kliebsiella pneumoniae, Pseudomonas aeruginosa, and Proteus vulgaris [27, 31]. B. grandiflora also possesses antioxidant, antidiabetic, anthelmintic, and analgesic properties [33, 34]. Its antimicrobial activity is attributed to Betulinic acid, a significant triterpenoid and active component of the plant [27, 29]. Furthermore, the plant contains bioactive constituents such as tannins, flavonoids, triterpenes, glycosides, and alkaloids [29, 33]. To the best of our knowledge, based on a literature search, there are few reports on the molecular docking of bioactive compounds from medicinal plants to the active site of MtDHFR. This study employs in-silico docking to evaluate the bioactive compounds in B. grandiflora and S. occidentalis for their potential to inhibit MtbDHFR.

MATERIALS AND METHODS

Plant Collection and Identification

Fresh leaves of B. grandiflora *and* S. occidentalis were collected from trees in Abuja Municipal Area Council, Federal Capital Territory, Nigeria. The plant species were identified and authenticated at the Herbarium Unit of the National Institute for Pharmaceutical Research and Development (NIPRD), Abuja, following standard taxonomic procedures [35]. Voucher specimens were deposited under the accession numbers NIPRD/H/7289 and NIPRD/H/7294.

Drying and Pulverization

To preserve phytochemical integrity, the collected plant materials were shade-dried at room temperature with periodic turning to ensure uniform drying, as previously described by [35]. Once completely dried, a wooden pestle and mortar were used to crush the plant material, and the powdered samples were weighed using an analytical scale before storage at room temperature.

Extract Preparation

Extraction was performed using the maceration technique, following the method outlined by [35]. Briefly, 500 g of dried plant powder was soaked in 2000 mL of 70% hydro-ethanol for 72 hours with intermittent agitation. The extract was filtered using Whatman No. 1 filter paper and concentrated under reduced pressure at 40°C using a rotary evaporator.

Fractionation of Extracts

The crude extract was fractionated using a solvent partitioning technique, previously described by [35]. Non-polar compounds were extracted with n-hexane, followed by ethyl acetate for semi-polar compounds, and the remaining aqueous fraction was freeze-dried.

Gas Chromatography-Mass Spectrometry (GC-MS) Analysis

GC-MS analysis of the extracts was conducted using an Agilent 7890A GC system equipped with a 5975C mass

ISSN No. 2454-6194 | DOI: 10.51584/IJRIAS |Volume X Issue III March 2025

spectrometer detector, following the procedure detailed in [35].

Selection of Ligands for *In-Silico* Study

Eight bioactive compounds with prominent peak area percentages from the GC-MS analysis were selected from the n-hexane fractions of B. grandiflora and S. occidentalis [35]. From the n-hexane fraction of B. grandiflora, the selected compounds included Palmitic acid, Phytol, Hexadecanoic acid ethyl ester, and Dichloroacetic acid tridec-2-ynyl ester. Meanwhile, the n-hexane fraction of S. occidentalis yielded, L-(+)-ascorbic acid 2,6-dihexadecanoate, Z-5,17-octadecadien-1-ol acetate, Phytol, Hexadecanoic acid ethyl ester, Butyl 9,12-octadecadienoate, and Ethyl 9,12,15-octadecatrienoate. Notably, Phytol and Hexadecanoic acid ethyl ester were present in both plants. Additionally, the therapeutic compound currently used for the treatment of TB, namely isoniazid, was also selected as the reference drug. The three-dimensional (3D) structures in structure data format (SDF) files, PubChem identification numbers (PIDs), and canonical SMILES of the selected bioactive compounds were retrieved from the PubChem database (https://pubchem.ncbi.nlm.nih.gov/compound/) (Table 2) [36].

Protein Targets Selection and Preparation

MtbDHFR (6VVB.pdb) was selected as the target protein [8, 37]. The three-dimensional (3D) crystallographic structure of the target protein (6VVB.pdb) was retrieved from the RCSB Protein Data Bank (www.rcsb.org) [38], and subsequently saved in PDB format (Fig. 1). The motif/complex was visualized in chimeraX and PyMol, and protein-ligand interaction was derived from PDBSum via LIGPLOT interactions. The target is an oxidoreductase obtained from Mycobacterium tuberculosis H37Rv, a widely used strain for genome reference sequencing. It was expressed on Escherichia coli BL21(DE3). X-ray Diffraction of the crystal lattice was obtained at 1.45 Å resolution.

Virtual Screening/Molecular Docking

Ligands and Protein targets for molecular docking were prepared in Autodock Tools using PyRx 0.8 package [39]. A grid box (x: 89.4261, y: 86.5813, z: 98.8772), dimensions (Angstrom) (x: 44.1528 y: 48.0231 z: 25.0000) was employed and docking simulations of bioactive conformations was done using Autodock Vina [40], and iGEMDOCK (Version2.1), a Graphical-Automatic Drug Design System for Docking, Screening and Post Analysis, from BioXGEM LAB [41]. The ligands were inputted as Standard Database Files (.sdf files) while the target protein was inputted as a Protein Database File (.pdb file) then converted to the acceptable Protein Data Bank, Partial Charge (Q), & Atom Type (T) format (. pdbqt file format) for Autodock Vina. Results obtained were analyzed using PyMol [42], and Discovery Studio 4.5 visualizer [43]. Standard docking was also performed with 200 population sizes, 70 generations, and 2 number of solutions each to determine the best pose(s) in the ligand binding cavity. The scores for the docking were generated based on the interaction profile/analysis, and correlated to those of the reference drugs used. The interaction energy between the ligand and receptor at the whole binding region was calculated and reported as affinity (kcal/mol).

RESULTS

The eight bioactive compounds and their peak area percentage are presented in table 1. Furthermore, the PubChem identification numbers (PIDs), and canonical SMILES of the selected bioactive compounds are shown in table 2.

Table 1: The Medicinal Plants and Bioactive Compounds used in Docking Studies

Medicinal Plants	Code	Bioactive Compounds	Peak % Area
Berlinia grandiflora	Compound 1	Palmitic acid	19.24
	Compound 2*	Hexadecanoic acid ethyl ester	9.02
	Compound 3*	Phytol	17.39
	Compound 4	Dichloroacetic acid tridec-2-ynyl ester	9.60
	Compound 5	L-(+)-ascorbic acid 2, 6-dihexadecanoate	15.30

ISSN No. 2454-6194 | DOI: 10.51584/IJRIAS |Volume X Issue III March 2025

Senna occidentalis			
	Compound 2*	Hexadecenoic acid ethyl ester	15.75
	Compound 3*	Phytol	15.57
	Compound 6	Z-5, 17-octadecadien-1-ol acetate	13.16
	Compound 7	Butyl 9, 12-octadecadienoate	9.09
	Compound 8	Ethyl 9, 12, 15-octadecatrienoate	13.51

*= Bioactive compounds present in both plants

Table 2: Library of selected plants, compounds and their canonical smiles

S/N	Plant	Name of Compound	ID	Canonical Smiles
1	Berlinia grandiflora	Palmitic acid	985	CCCCCCCCCCCCCCCC(=O)O
		Hexadecanoic acid ethyl ester	12366	CCCCCCCCCCCCCCCC(=O)OCC
		Phytol	5280435	CC(C)CCCC(C)CCCC(C)CCCC(=CCO)C
		Dichloroacetic acid tridec-2-ynyl ester	531238	CCCCCCCCCCC#CCOC(=O)C(Cl)Cl
2	Senna occidentalis	L-(+)-ascorbic acid 2, 6-dihexadecanoate	54722209	CCCCCCCCCCCCCCCC(=O)OCC(C1C(=C(C(=O)O1)OC(=O)CCCCCCCCCCCCCCC)O)O
		Hexadecenoic acid ethyl ester	12366	CCCCCCCCCCCCCCCC(=O)OCC
		Phytol	5280435	CC(C)CCCC(C)CCCC(C)CCCC(=CCO)C
		Z-5, 17-octadecadien-1-ol acetate	5363494	CC(=O)OCCCCC=CCCCCCCCCCCC=C
		Butyl 9, 12-octadecadienoate	102296	CCCCCC=CCC=CCCCCCCCC(=O)OCCCC
		Ethyl 9, 12, 15-octadecatrienoate	6371716	CCC=CCC=CCC=CCCCCCCCC(=O)OCC

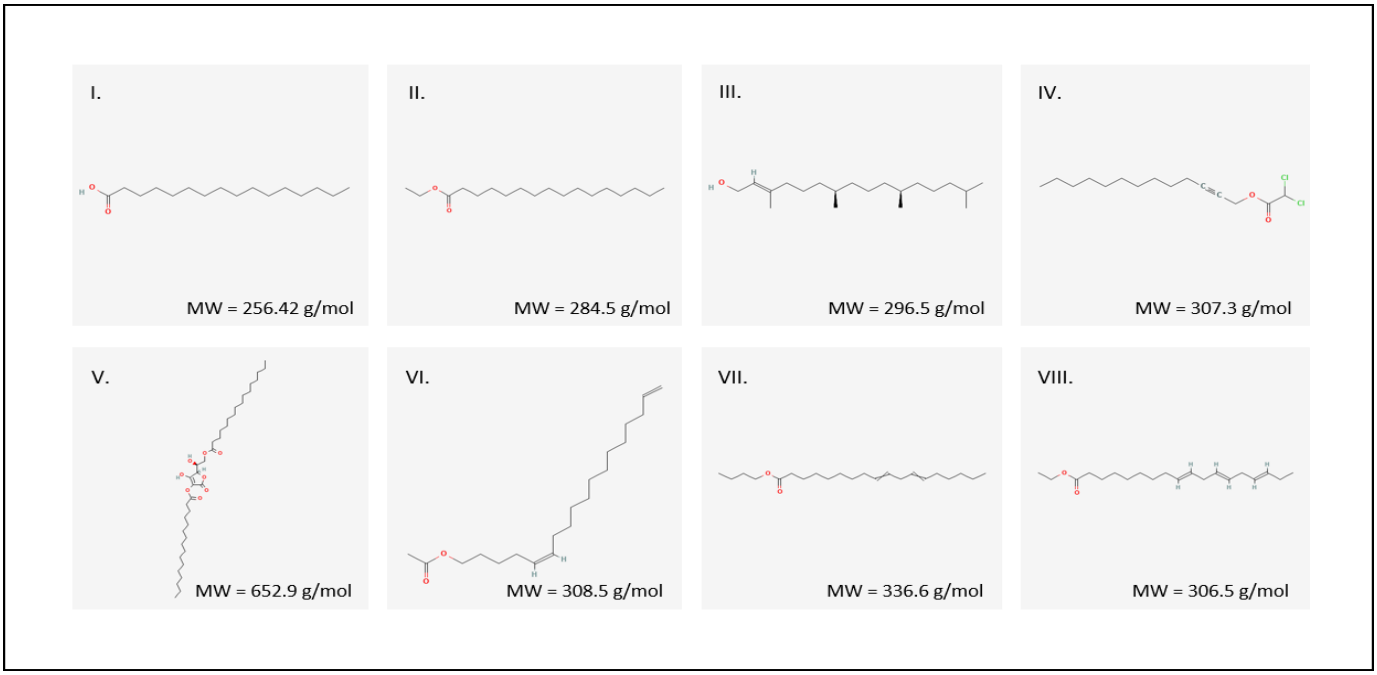

Figure 1: Chemical structures of the bioactive compounds used for the *in-silico* screening and their molecular weights (MW).

ISSN No. 2454-6194 | DOI: 10.51584/IJRIAS |Volume X Issue III March 2025

(I) Palmitic acid (MW = 256.42 g/mol); (II) Hexadecanoic acid ethyl ester (MW = 284.5 g/mol); (III) Phytol (MW = 296.5 g/mol); (IV) Dichloroacetic acid tridec-2ynyl ester (MW = 307.3 g/mol); (V) L- (+) ascorbic acid 2, 6-dihexadecanoate (MW = 652.9 g/mol); (VI) Z-5, 17-octadecadien-1-ol acetate (MW = 308.5 g/mol); (VII) Butyl 9, 12-octadecadienoate (MW = 336.6 g/mol); and (VIII) Ethyl 9, 12, 15-octadecatrienoate (MW = 306.5 g/mol) (Adopted from Pubchem).

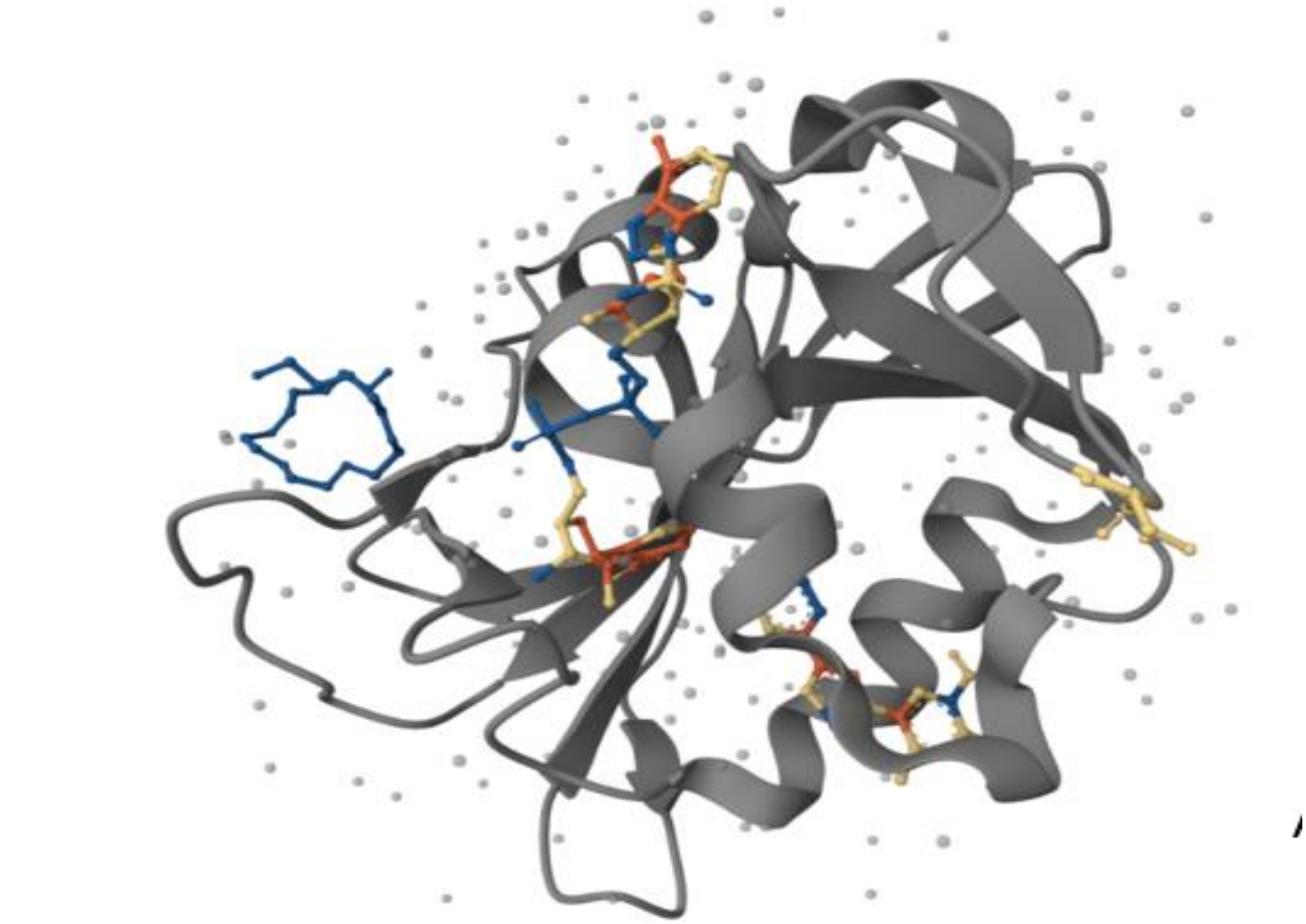

Figure 2: Crystal structure of *Mtb*DHFR with attached ligand and water molecules (Retrieved from RCSB Protein Data Bank).

Virtual screening

The analyzed virtual screening results of the binding energies (kcal/mol) of the bioactive compounds contained in the plant constituents of B. grandiflora and S. occidentalis to MtbDHFR molecular target (6VVB.pdb) were ranked and are presented in Table 3. The molecular docking results revealed that the binding energies of the bioactive compounds range between -4.468 and -6.146 kcal/mol, while the reference drug exhibited a binding energy of -5.392 kcal/mol. Compound 5 (L-(+)-ascorbic acid 2, 6-dihexadecanoate), exhibited the highest binding energy of -6.146 kcal/mol whereas Compound 1 (Palmitic acid), showed the lowest binding energy of -4.468 kcal/mol. Hexadecanoic acid ethyl ester and Phytol, present in both plants, exhibited binding energies of -5.281 and -5.379 kcal/mol, respectively. Dichloroacetic acid tridec-2-ynyl ester, present in B. grandiflora, exhibited a binding energy of -5.490 kcal/mol. L-(+)-ascorbic acid 2, 6-dihexadecanoate, Z-5, 17-Octadecadien-1-ol acetate, Butyl 9, 12-octadecadienoate, and Ethyl 9, 12, 15-octadecatrienoate have been identified as bioactive compounds in S. occidentalis. They exhibited binding energies of - 6.146, -5.558, - 5.652, and -5.485 kcal/mol, respectively.

ISSN No. 2454-6194 | DOI: 10.51584/IJRIAS |Volume X Issue III March 2025

Table 3: Molecular interactions of the bioactive compounds and the reference drug with the target protein MtbDHFR (6VVB.pdb) active site.

Bioactive Compounds	**Binding Energy (Kcal/mol)**	**Rank**	**Residues involved in hydrophobic interaction(Å)**	
Compound 5	- 6.146	1	Lys53, Asp27, Try100, Thr113	Phe31, Ile5, Trp6, Ile14
Compound 7	- 5.652	2	Asp27, Thr113, Ile20	Phe31, Ile5, Thr46, Trp6, Ile16
Compound 6	-5.558	3	Asp27, Thr113, His30	Ile5, Thr6, Trp6
Compound 4	- 5.490	4	Asp27, Thr113, Thr46	His30, Ile15, Thr46, Trp6, Ile14
Compound 8	- 5.485	5	Lys53, Trp6, Ala7, Asp27	Arg55, Phe13, Ile94
Compound 3	- 5.379	6	Asp27, Ile94, Gly95, Try100	Phe31, Ile20, Thr46
Compound 2	- 5.281	7	Asp27, Thr113	His30, Ile5, Trp6
Compound 1	- 4.468	8	Asp27, Thr113, Trp6	Thr46
Isoniazid	- 5.392		Asp27, Try100, Gly95, Glu30	Phe31, Ile5, Leu28

Binding Interactions

All the molecules used in the study were observed to have docked properly in the active site of the target. Upon binding of the molecules to 6VVB.pdb, no global changes were observed. Figures 3a-3h, shows the binding interactions and conformations of the bioactive compounds in the medicinal plants on the active site residues of *Mtb*DHFR (6VVB.pdb).

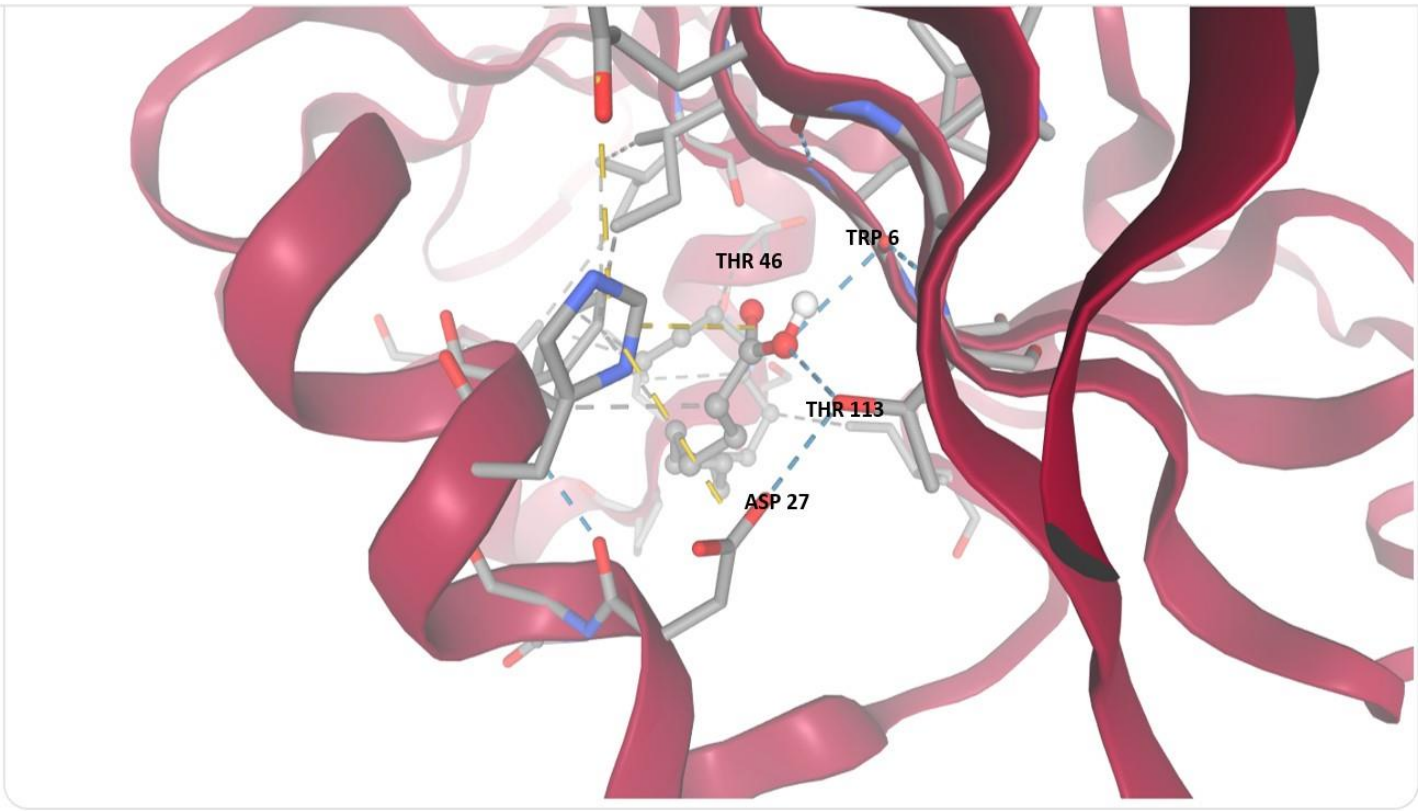

ISSN No. 2454-6194 | DOI: 10.51584/IJRIAS |Volume X Issue III March 2025

Fig 3a: 3D binding interactions of compound 1 (Palmitic acid) docked to the 6VVB binding cavity of MtbDHFR.

Ligands are shown in ball and stick forms while amino acid residues are shown in stick forms. Hydrogen-bond interaction with amino acid main chains are indicated by blue discontinuous lines, gray-colored discontinuous lines show hydrophobic interactions while yellow lines show ionic interactions.

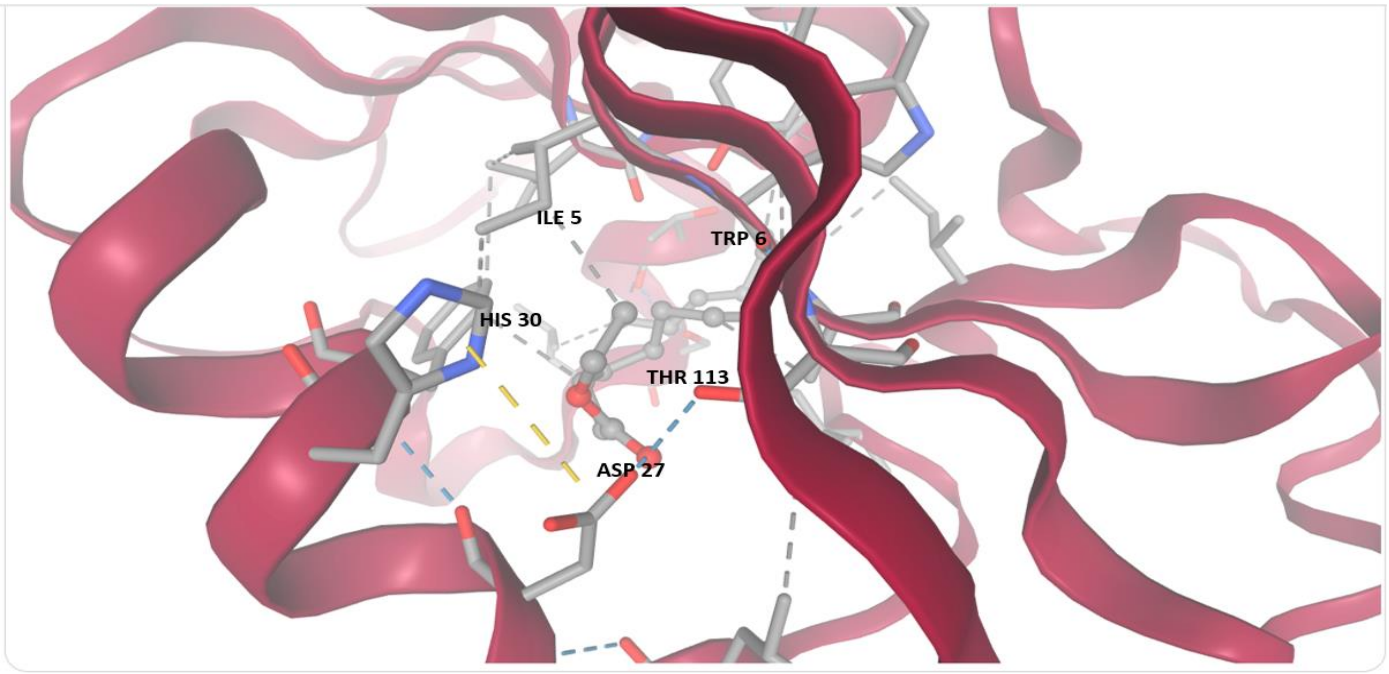

Fig 3b: 3D binding interactions of compound 2 (Hexadecanoic acid ethyl ester) docked to the 6VVB binding cavity of *Mtb*DHFR.

Ligands are shown in ball and stick forms while amino acid residues are shown in stick forms. Hydrogen-bond interaction with amino acid main chains are indicated by blue discontinuous lines, gray-coloured discontinuous lines show hydrophobic interactions while yellow lines show ionic interactions.

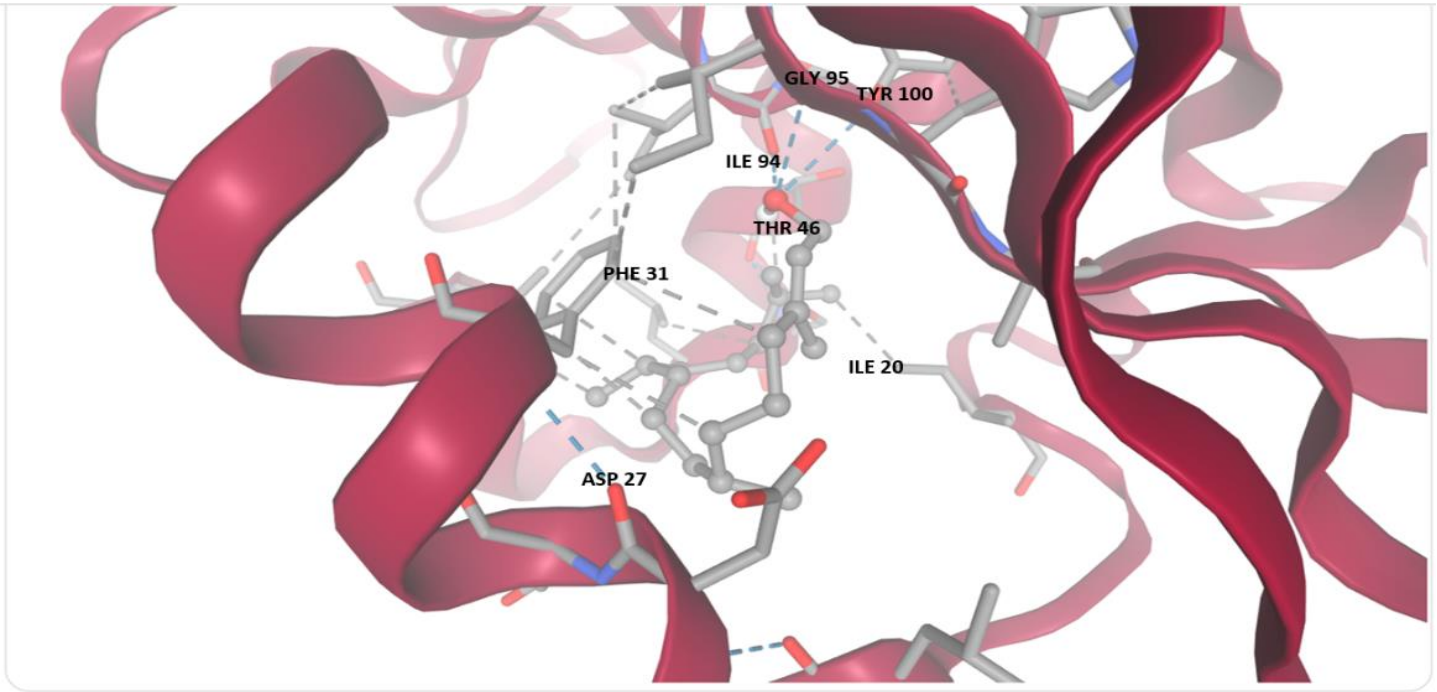

Fig 3c: 3D binding interactions of compound 3 (Phytol) docked to the 6VVB binding cavity of MtbDHFR.

ISSN No. 2454-6194 | DOI: 10.51584/IJRIAS |Volume X Issue III March 2025

Ligands are shown in ball and stick forms while amino acid residues are shown in stick forms. Hydrogen-bond interaction with amino acid main chains is indicated by blue discontinuous lines, gray-coloured discontinuous lines show hydrophobic interactions while yellow lines show ionic interactions.

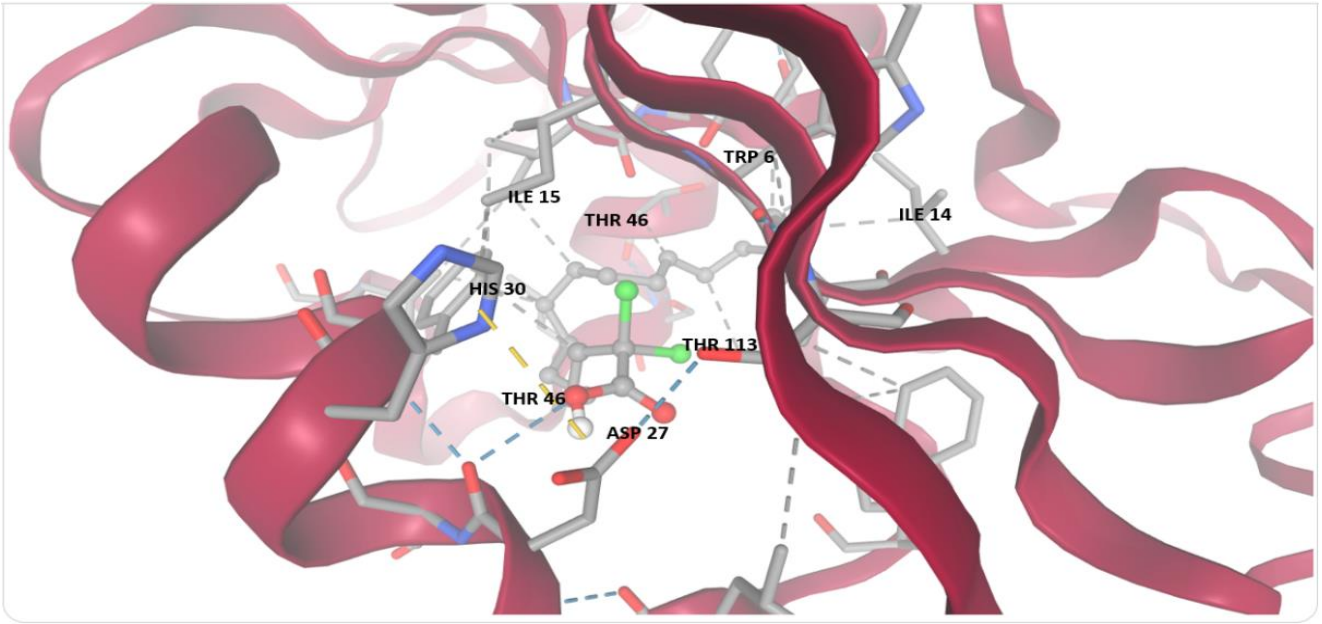

Fig 3d: 3D binding interactions of compound 4 (Dichloroacetic acid tridec-2-ynyl ester) docked to the 6VVB binding cavity of *Mtb*DHFR.

Ligands are shown in ball and stick forms while amino acid residues are shown in stick forms. Hydrogen-bond interaction with amino acid main chains are indicated by blue discontinuous lines, gray-coloured discontinuous lines show hydrophobic interactions while yellow lines show ionic interactions.

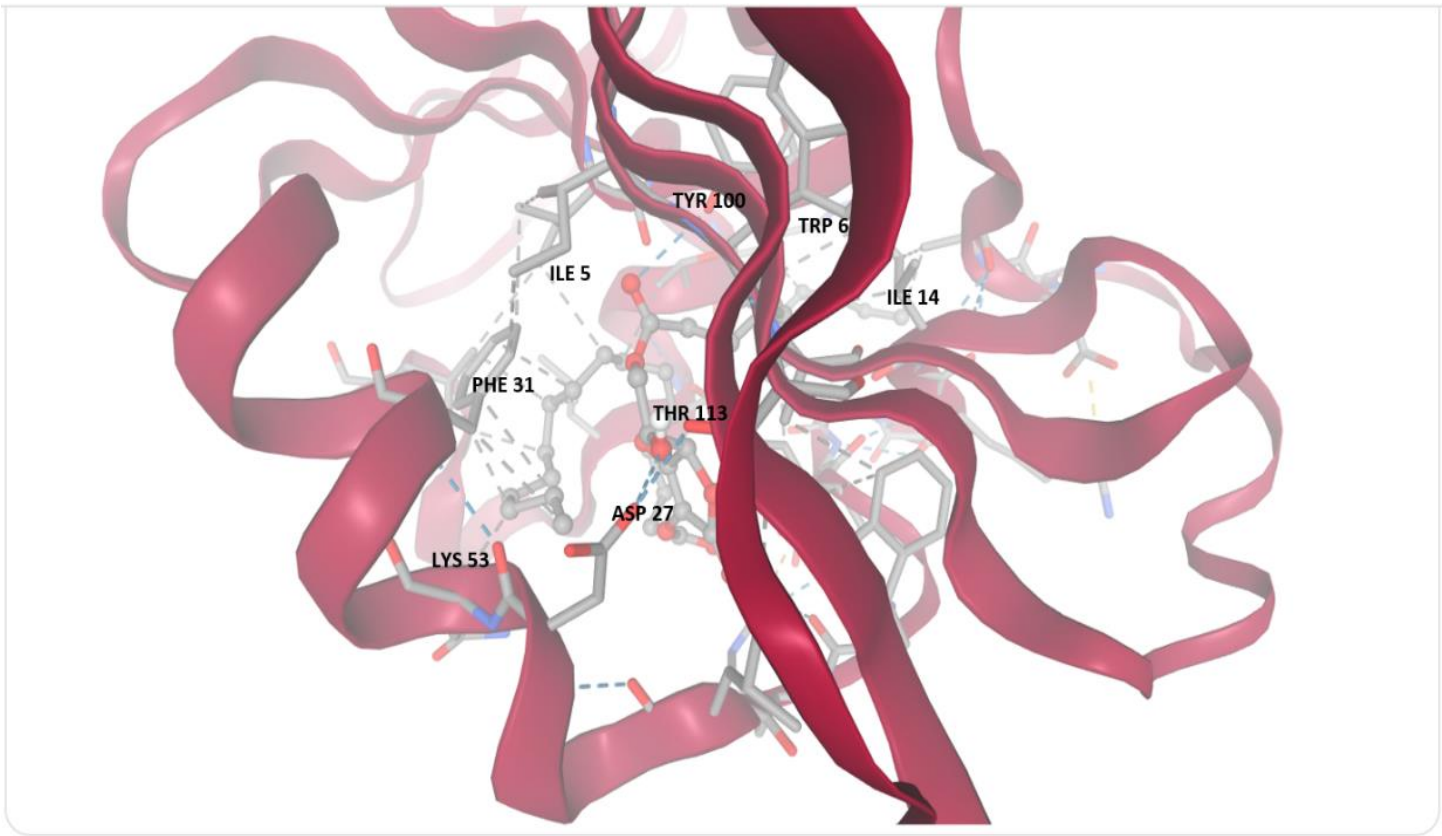

Fig 3e: 3D binding interactions of compound 5 (L-(+)-ascorbic acid 2, 6-dihexadecanoate) docked to the 6VVB binding cavity of MtbDHFR.

ISSN No. 2454-6194 | DOI: 10.51584/IJRIAS |Volume X Issue III March 2025

Ligands are shown in ball and stick forms while amino acid residues are shown in stick forms. Hydrogen-bond interaction with amino acid main chains are indicated by blue discontinuous lines, gray-coloured discontinuous lines show hydrophobic interactions while yellow lines show ionic interactions.

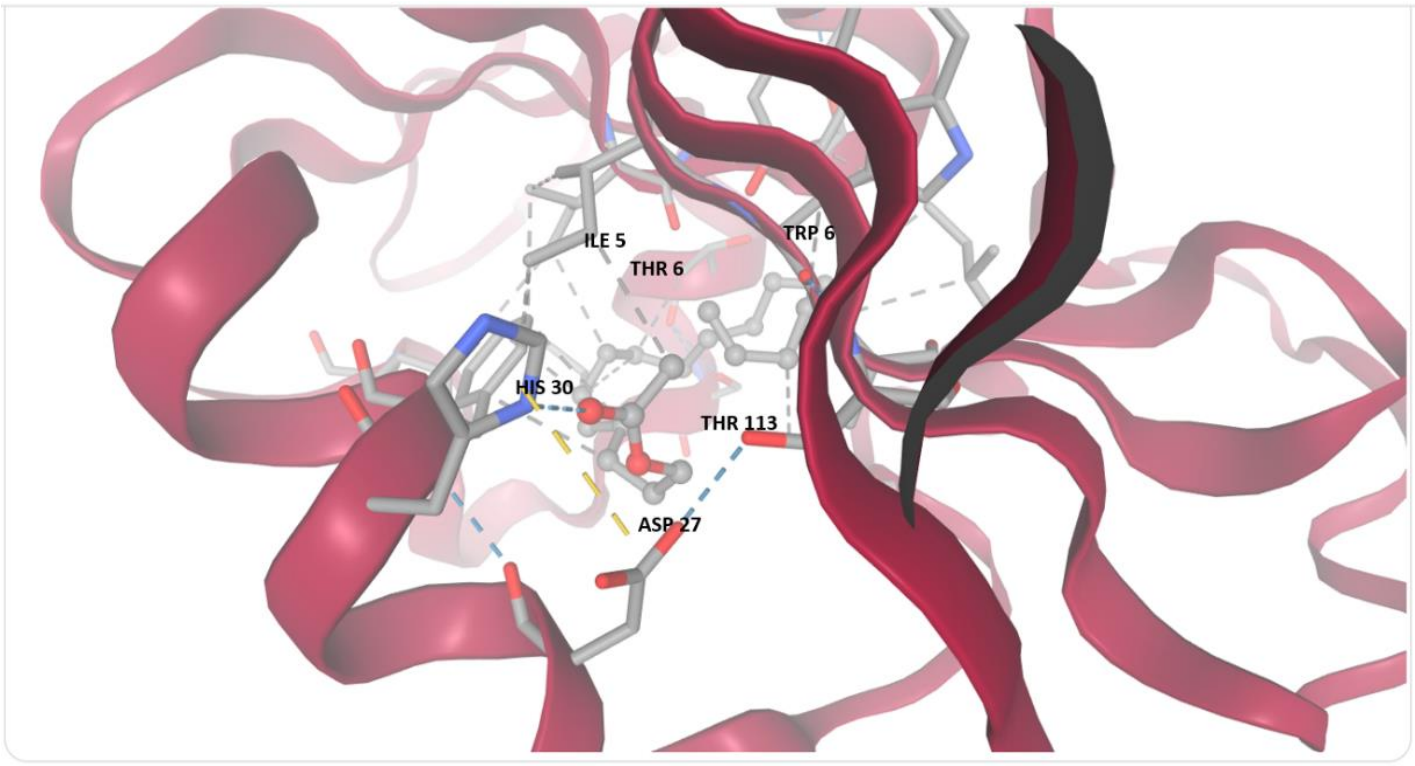

Fig 3f: 3D binding interactions of compound 6 (Z-5, 17-octadecadien-1-ol acetate) docked to the 6VVB binding cavity of *Mtb*DHFR.

Ligands are shown in ball and stick forms while amino acid residues are shown in stick forms. Hydrogen-bond interaction with amino acid main chains are indicated by blue discontinuous lines, gray-coloured discontinuous lines show hydrophobic interactions while yellow lines show ionic interactions.

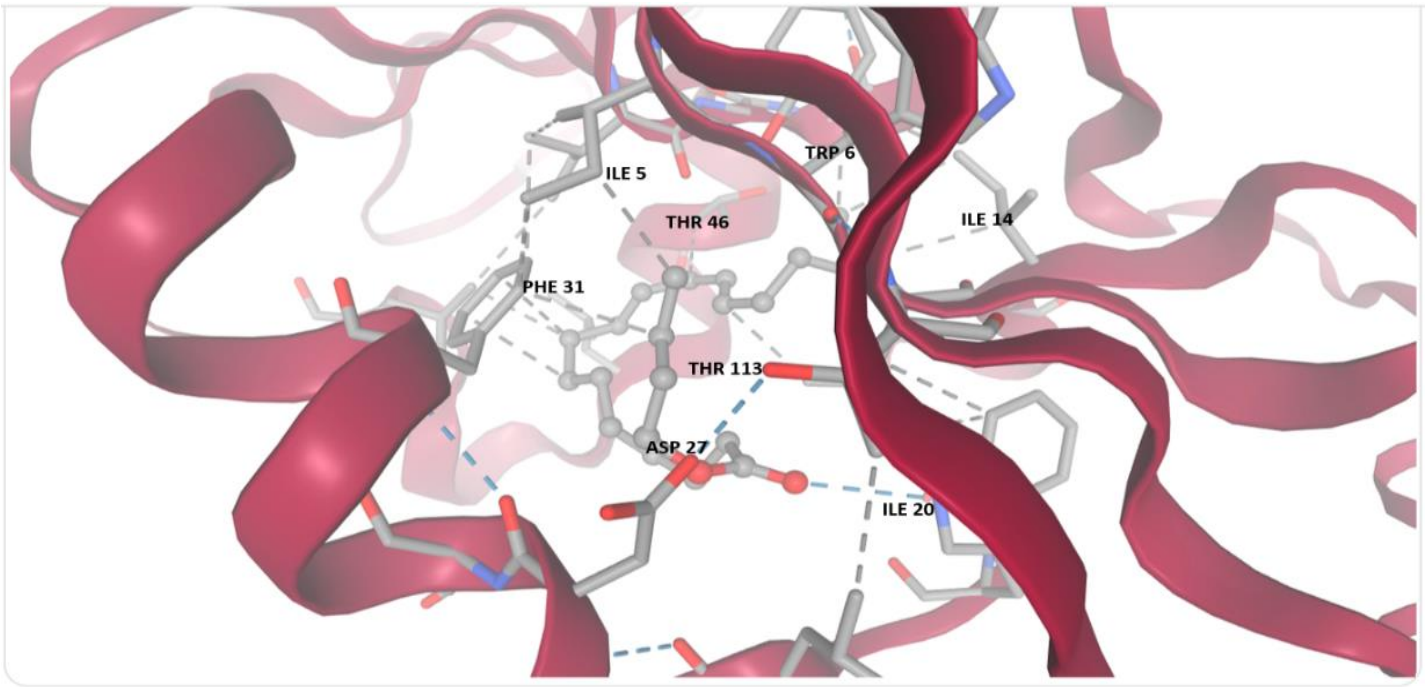

Fig 3g: 3D binding interactions of compound 7 (Butyl 9, 12-octadecadienoate) docked to the 6VVB binding cavity of MtbDHFR.

ISSN No. 2454-6194 | DOI: 10.51584/IJRIAS |Volume X Issue III March 2025

Ligands are shown in ball and stick forms while amino acid residues are shown in stick forms. Hydrogen-bond interaction with amino acid main chains are indicated by blue discontinuous lines, gray-coloured discontinuous lines show hydrophobic interactions while yellow lines show ionic interactions.

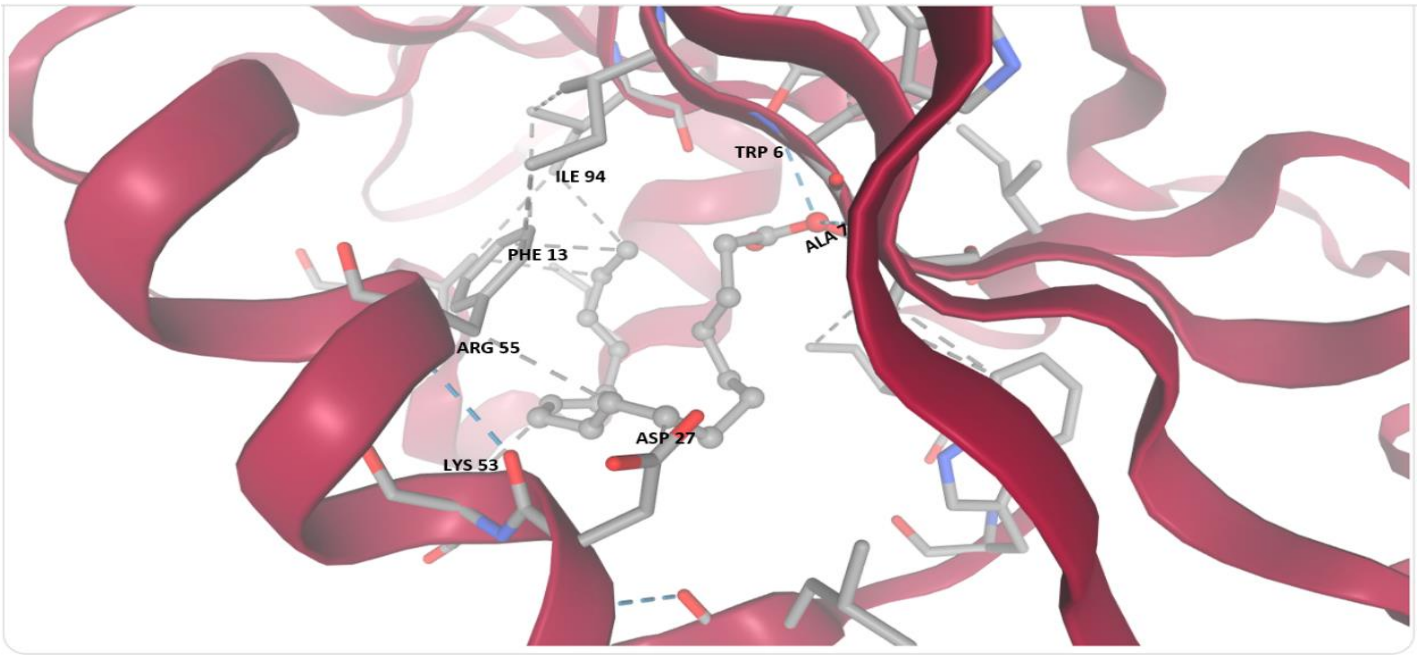

Fig 3h: 3D binding interactions of compound 8 (Ethyl 9, 12, 15-octadecatrienoate) docked to the 6VVB binding cavity of MtbDHFR.

Ligands are shown in ball and stick forms while amino acid residues are shown in stick forms. Hydrogen-bond interaction with amino acid main chains are indicated by blue lines, gray-coloured discontinuous lines show hydrophobic interactions while yellow lines show ionic interactions.

DISCUSSION

The shape and electrostatic relationships between the ligand and protein can be understood through their binding interactions. Additionally, molecular docking predicts how the ligand will attach to residues in the enzyme's active site, as well as the ligand's orientation and conformation within the protein's binding pocket. The overall interaction energy is represented by the docking score, where stronger interactions are indicated by lower negative values [44]. [35], presented the chromatogram of the selected bioactive compounds in their study. The 3D binding interactions of the bioactive compounds, namely Palmitic acid, Hexadecanoic acid ethyl ester, Phytol, Dichloroacetic acid tridec-2-ynyl ester, L-(+)-ascorbic acid 2,6-dihexadecanoate, Z-5,17-octadecadien-1-ol acetate, Butyl 9,12-octadecadienoate, and Ethyl 9,12,15-octadecatrienoate, to the active site residues of *Mtb*DHFR (6VVB.pdb) are presented in Figures 3a–3h. These interactions include binding energy, binding efficiency, hydrophobic interactions, and hydrogen bonding interactions. Binding pattern analysis (Figure 3) revealed numerous hydrogen-bond and hydrophobic interactions. Figures 3a–3h showed the three-dimensional images of the binding, indicating that the compounds or ligands occupy identical active site pockets. This could be attributed to the crystal structure of *Mtb*DHFR having a well-defined binding site. The conformation seen in Figures 3d–3g indicates that the ligands are buried in a significantly deeper pocket within the protein target.

A previous study by [35], showed that the n-hexane fractions of both plants exhibited the best anti-TB activity compared to the ethyl acetate and aqueous fractions. The hexane fraction of S. occidentalis displayed the lowest MIC (156 µg/mL) and MBC (313 µg/mL) against M. tuberculosis. Similarly, the hexane fraction of B. grandiflora exhibited the lowest MIC (313 µg/mL) and MBC (625 µg/mL) against M. tuberculosis. As seen in Table 3, some bioactive compounds found in B. grandiflora and S. occidentalis had stronger binding energies for the target compared to the reference drug, Isoniazid. A study by [45], revealed that the acyclic 4R isomer of isoniazid-NADP inhibits MtbDHFR, an enzyme essential for nucleic acid synthesis.

ISSN No. 2454-6194 | DOI: 10.51584/IJRIAS |Volume X Issue III March 2025

This study highlighted Compound 5 [L-(+)-ascorbic acid 2,6-dihexadecanoate], derived from S. occidentalis, as the compound with the best binding energy (-6.146 kcal/mol) among all the docked compounds (Table 3), with most of its hydrogen bond lengths being shorter compared to the other compounds (Figure 3e). The compound with the lowest binding affinity was Compound 1 (Palmitic acid) from B. grandiflora, exhibiting a binding energy of -4.468 kcal/mol. Five compounds (Compounds 4–8) present in the plants had stronger binding energies than the reference drug included in this computational evaluation (Table 3), suggesting their potential to inhibit the activity of M. tuberculosis and serve as possible anti-TB agents. A study by [46], also demonstrated the molecular docking of compounds found in Piper betle leaves (Phytol, Chavibetol, Hydroxychavicol) on MtbDHFR, with binding energies of -5.07, -5.17, and -5.26 kcal/mol, respectively.

Binding of bioactive compounds to the MtbDHFR target offers promising anti-tubercular potential by inhibiting the enzyme's activity. The apparent ability of these compounds to bind to the enzyme's catalytic sites suggests their potential as inhibitors. The investigated compounds exhibited higher binding energies to MtbDHFR than the reference drug, reinforcing their potential as anti-tuberculosis agents. The ligand L-(+)-ascorbic acid 2,6-dihexadecanoate, which demonstrated the highest docking score, showed strong binding energy to specific amino acid residues. It formed hydrogen interactions with Lys53, Asp27, Tyr100, and Thr113, while hydrophobic interactions were observed with Phe31, Ile5, Trp6, and Ile14. Similarly, Butyl 9,12-octadecadienoate formed hydrogen bonds with Asp27, Thr113, and Ile20, along with hydrophobic interactions involving Phe31, Ile5, Thr46, Trp6, and Ile16. Dichloroacetic acid tridec-2-ynyl ester formed hydrogen bonds with Asp27, Thr113, and Thr46, as well as hydrophobic interactions with His30, Ile15, Thr46, Trp6, and Ile14. Z-5,17-octadecadien-1-ol acetate exhibited hydrogen bonding with Asp27, Thr113, and His30, and hydrophobic interactions with Ile5, Thr6, and Trp6. Ethyl 9,12,15-octadecatrienoate exhibited hydrogen interactions with Lys53, Trp6, Ala7, and Asp27, as well as hydrophobic interactions with Arg55, Phe13, and Ile94. Phytol formed hydrogen bonds with Asp27, Ile94, Gly95, and Tyr100, and hydrophobic interactions with Phe31, Ile20, and Thr46. Palmitic acid exhibited hydrogen interactions with Asp27, Thr113, and Trp6, along with hydrophobic interactions with Thr46. Similarly, Hexadecanoic acid ethyl ester showed hydrogen interactions with Asp27 and Thr113, as well as hydrophobic interactions involving His30, Ile5, and Trp6. Collectively, these residues form a binding pocket for the ligands, indicating their ability to interfere with M. tuberculosis resistance mechanisms.

The pharmacological properties of a drug are demonstrated by its capacity to bind to biological targets, including ion channels, enzymes, and receptors [47]. This research indicates that all the compounds, except Compound 1 (Palmitic acid), along with the reference drug, Isoniazid, had bioactivity scores greater than −5.0 (> -5.0). This suggests that they are actively involved in binding to nuclear receptor ligands and G protein-coupled receptors (GPCRs), modulating ion channels, and inhibiting kinases, proteases, and enzymes. The findings of this study suggest that the selected bioactive compounds in the studied medicinal plants particularly, Palmitic acid, Hexadecanoic acid ethyl ester, Phytol, Dichloroacetic acid tridec-2-ynyl ester, L-(+)-ascorbic acid 2,6-dihexadecanoate, Z-5,17-octadecadien-1-ol acetate, Butyl 9,12-octadecadienoate, and Ethyl 9,12,15-octadecatrienoate exhibit an in-silico inhibitory effect against MtbDHFR through molecular docking techniques. These results provide valuable insights for the development of potent drug formulations, selection of promising compounds, and assurance of patient safety. Overall, this in-silico investigation offers a promising avenue for developing new plant-based anti-TB agents that could complement existing treatment regimens and help combat drug-resistant strains of M. tuberculosis.

CONCLUSIONS

The molecular docking analysis of the bioactive compounds derived from the medicinal plants demonstrates promising inhibitory potential against *Mtb*DHFR (6VVB.pdb), an enzyme crucial for bacterial survival and replication. The study highlights that these bioactive compounds exhibit high binding energies to *Mtb*DHFR, compared to the reference drug used in the treatment of TB. These findings identify the bioactive compounds as viable candidates for further preclinical testing and emphasize the value of computational approaches in accelerating drug discovery. However, the results should be validated through *in-vitro* and *in-vivo* studies to confirm biological efficacy and safety of these compounds. Additionally, ADMET (Absorption, Distribution, Metabolism, Excretion, and Toxicity) profiling and structure-activity relationship (SAR) analysis will be crucial in optimizing the lead compounds for clinical applications. By integrating *in-silico* predictions with experimental validations, this research could pave the way for novel, effective, and safer TB treatment strategies.

Declaration of competing interest

The authors declare that they have no known competing financial interests or personal relationships that could have appeared to influence the work reported in this paper.

REFERENCES

1. Chaisson, R. E., Frick, M., & Nahid, P. (2022). The scientific response to TB – the other deadly global health emergency. Int. J. Tuberc. Lung. Dis., 6(3), 186–189. https://doi.org/10.5588/ijtld.21.0734.
2. World Health Organization Global Tuberculosis Report 2023. World Health Organization; Geneva, Switzerland: https://www.who.int/news-room/fact-sheets/detail/tuberculosis.
3. Li, L., Abdurahman, Z., Zhong, X., Gong, H., Yang, F., Awuti, A., Alimu, A., Yilamujiang, S., Zheng, D., & Zou, X. (2023). Clinical symptoms and immune injury reflected by low CD4/CD8 ratio should increase the suspicion of HIV coinfection with tuberculosis. Heliyon, 9(3), e14219. https://doi.org/10.1016/j.heliyon.2023.e14219.
4. Sun, L., Chen, Y., Yi, P., Yang, L., Yan, Y., Zhang, K., Zeng, Q., & Guo, A. (2021). Serological Detection of Mycobacterium Tuberculosis Complex Infection in Multiple Hosts by One Universal ELISA. PLoS One, 16(10), 920–938. https://doi.org/10.1371/journal.pone.0257920.
5. García, J. I., Allué-Guardia, A., Tampi, R. P., Restrepo, B. I., & Torrelles, J. B. (2021). New Developments and Insights in the Improvement of Mycobacterium Tuberculosis Vaccines and Diagnostics Within the End TB Strategy. Curr. Epidemiol. Report, 8, 33–45. https://doi.org/10.1007/s40471-021-00269-2.
6. Khawbung, J. L., Nath, D., & Chakraborty, S. (2021). Drug resistant Tuberculosis: A review. Comparative Immunology, Microbiology and Infectious Diseases, 74, 574–583. https://doi.org/10.1016/j.cimid.2020.101574.
7. Farjallah, A., Chiarelli, L. R., Forbak, M., Degiacomi, G., Danel, M., Goncalves, F., & Chassaing, S. (2021). A coumarin-based analogue of thiacetazone as dual covalent inhibitor and potential fluorescent label of HadA in Mycobacterium tuberculosis. ACS. Infect. Dis., 7(3), 552–565. https://doi.org/10.1021/acsinfecdis.0c00325.
8. Vassiliades, S. V., Navarausckas, V. B., Dias, M. V. B., & Parise-Filho, R. (2023). Mycobacterium tuberculosis Dihydrofolate Reductase Inhibitors: State of Art Past 20 Years. Biointerface Research in Applied Chemistry, 13(1), 79. https://doi.org/10.33263/BRIAC131.079.
9. Kirkman, T., Suk Fun Tan, S. F., Chavez-Pacheco, S. M., Hammer, A., Abell, C., Tosin, M., Coyne, A. G., & Dias, M. V. B. (2023). Fragment-Merging Strategies with Known Pyrimidine Scaffolds Targeting Dihydrofolate Reductase from Mycobacterium tuberculosis. Chem. Med. Chem., 18, e202300240. https://doi.org/10.1002/cmdc.202300240.
10. He, J., Qiao, W., An, Q., Yang, T., & Luo, Y. (2020). Dihydrofolate reductase inhibitors for use as antimicrobial agents. European Journal of Medicinal Chemistry, 195, 112268. https://doi.org/10.1016/j.ejmech.2020.112268.
11. Minato, Y., Gohl, D. M., Thiede, J. M., Chacón, J. M., Harcombe, W. R., Maruyama, F., & Baughn, A. D. (2019). Genome wide Assessment of Mycobacterium tuberculosis Conditionally Essential Metabolic Pathways. mSystems, 4(4), 1–13. https://doi.org/10.1128/msystems.00070- 19.
12. Sharma, M., & Chauhan, P. M. S. (2012). Dihydrofolate Reductase as a Therapeutic Target for Infectious Diseases: Opportunities and Challenges. Future Med. Chem., 4(10), 1335–1365. https://doi.org/10.4155/fmc.12.68.
13. Nixon, M. R., Saionz, K. W., Koo, M. S., Szymonifka, M. J., Jung, H., Roberts, J. P., Nandakumar, M., Kumar, A., Liao, R., & Rustad, T. (2014). Folate pathway disruption leads to critical disruption of methionine derivatives in mycobacterium tuberculosis. Chem. Biol., 21(7), 819–830. https://doi.org/10.1016/j.chembiol.2014.04.009.
14. Gupta, V. K., Kumar, M. M., Bishta, D., & Kaushik, A. (2017). Plants in our combating strategies against Mycobacterium tuberculosis: progress made and obstacles met. Pharm Bio., 55(1), 1536–1544. https://doi.org/10.1080/13880209.2017.1309440.

15. Davies-Bolorunduro, O. F., Ajayi, A., Adeleye, I. A., Kristanti, A. N., & Aminah, N. S. (2021). Bioprospecting for antituberculosis natural products – A review. Open Chemistry, 19(1), 1074– 1088. https://doi.org/10.1515/chem-2021-0095.
16. Obakiro, S. B., Kiprop, A., K'owino, I., Andima, M., Owor, R. O., Chacha, R., & Kigondu, E. (2022). Phytochemical, Cytotoxicity, and Antimycobacterial Activity Evaluation of Extracts and Compounds from the Stem Bark of Albizia coriaria Welwex. Oliver. Evidence-Based Complementary and Alternative Medicine, 4, 7148511. https://doi.org/10.1155/2022/7148511.
17. Oryema, C., Rutaro, K., Oyet, S. W., & Malinga, G. M. (2021). Ethnobotanical plants used in the management of symptoms of tuberculosis in rural Uganda. Trop. Med. Health, 49(1), 92. https://doi.org/10.1186/s41182-021-00384-2.
18. Getachew, S., Medhin, G., Asres, A., Abebe, G., & Ameni, G. (2022). Traditional medicinal plants used in the treatment of tuberculosis in Ethiopia: A systematic review. Heliyon, 18(5), e09478. https://doi.org/10.1016/j.heliyon.2022. e09478.
19. Swain, S. S., Hussain, T., & Pati, S. (2021). Drug-lead anti-tuberculosis phytochemicals: A Systematic Review. Curr. Top. Med. Chem., 21(20), 1832–1868. https://doi.org/10.2174/1568026621666210705170510.
20. Usman, M. M., Aisami, A., Mohammed, S., & Sa'idu, H. (2023). African Medicinal Plants with Anti mycobacterium tuberculosis activity: A Review. Bima Journal of Science and Technology, 7(2), 18-29. https://doi.org/10.56892/bima.v7i2.422.
21. Scheidegger, N. M. B., & Rando, J. G. (2020). Cassia in Flora e Funga do Brasil 2020. Jardim Botânico do Rio de Janeiro. https://floradobrasil2020.jbrj.gov.br/FB22858.
22. da Silva Luna, V., Randau, K. P., Ferreira, M. R. A., & Soares, L. A. L. (2022). Development and validation of analytical method by spectrophotometry UV-Vis for quantification of flavonoids in leaves of Senna occidentalis Linn. Research, Society and Development, 11(1), e14411118584. https://doi.org/10.33448/rsd-v11i1.18584.
23. Waziri, A. F., & Bashir, K. A. (2022). The Competitive Ability of Senna occidentalis (Coffee Senna) among some Weedy Plant Species in Sokoto, Semi-Arid Ecological Zone, Nigeria. Direct Res. J. Biol. Biotechnol., 8(4), 29-33. https://doi.org/10.26765/DRJBB0176329548.
24. Nde, A. L., Chukwuma, C. I., Erukainure, O. L., Chukwuma, M. S., & Matsabisa, M. G. (2022). Ethnobotanical, phytochemical, toxicology and anti-diabetic potential of Senna occidentalis (L.) link; A review. Journal of Ethnopharmacology, 283, 114663. https://doi.org/10.1016/j.jep.2021.114663.
25. Durgapal, D., Singh, R., Padiyar, S. V. S., & Durgapal, P. (2023). Review Paper on Qualitative Analysis of Phytochemicals of Cassia occidentalis linn. Eur. Chem. Bull., 12(10), 4196- 4202. https://doi.org/10.48047/ecb/2023.12.si10.00482.
26. Issa, T. O., Mohamed Ahmed, A. I., Mohamed, Y. S., Yagi, S., Makhawi, A. M., & Khider, T. O. (2020). Physiochemical, Insecticidal, and Antidiabetic Activities of Senna occidentalis Linn Root. Biochem. Res. Int., 2020, 8810744. https://doi.org/10.1155/2020/8810744.
27. Adamu, A., Esievo, K. B., Ugbabe, G., Okhale, S. E., & Egharevba, H. O. (2018). High-performance liquid chromatography-diode array detection (HPLC-DAD) profiling, antioxidant and antiproliferative activities of ethanol leaf extract of Berlinia grandiflora (Vahl) Hutch. & Dalziel. Journal of Pharmacognosy and Phytotherapy, 10(11), 187-194. https://doi.org/10.5897/JPP2018.0524.
28. Akuodor, G. C., Onyewenjo, S. C., Anyalewechi, N. A., Essien, A. D., Akpan, J. L., Okoroafor, D. O., & Okere, M. O. (2011). In vitro antimicrobial activity of leaf extract of Berlina grandiflora Hutch. and Dalz. African Journal of Microbiology Research, 5(11), 1358-1360. https://doi.org/10.5897/AJMR10.692.
29. Aboaba, S., & Ibitoye, M. (2018). Chemical Composition and Toxicity Profile of the Essential Oils of Bosqueia angolensis Ficalho and Berlinia grandiflora (Vahl) Hutch & Dalziel. Research & Reviews: A Journal of Toxicology, 8(2), 15-20.
30. Timothy, U. J., Ankah, N. K., Umoren, P. S., Solomon, M. M., Igwe, I. O., & Umoren, S. A. (2023). Assessment of Berlinia grandiflora and cashew natural exudate gums as sustainable corrosion inhibitors for mild steel in an acidic environment. Journal of Environmental Chemical Engineering, 11(6), 111578. https://doi.org/10.1016/j.jece.2023.111578.

31. Joseph, G. C., Ching, F. P., & Nnabuife, A. C. (2012). Investigation of the antimicrobial potentials of some phytochemical extracts of leaf and stem bark of Berlinia grandiflora (Leguminoceae) Caesalpinioidae) against pathogenic bacteria. Afr. J. Pharmacol. Ther., 1(3), 92-96.
32. Ode, J., Nwaehujor, C. O., & Nwinyi, C. F. (2013). Evaluation of the antidiabetic and antioxidant activity of the methanol leaf extract of Berlinia grandiflora. Journal of Medical Sciences, 13(8), 743-748. https://doi.org/10.3923/jms.2013.743.748.
33. Donkor, M. N., Ayikanle, S. Y., & Donkor, S. A. (2018). Effect of Ethanol Stem Bark Extract of Berlinia grandiflora Hutch and Dalz on Marker Liver Enzymes in Rats Treated with CCl_4. Int. J. Pharm. Sci., 10(10), 69-73. https://doi.org/10.22159/ijpps.2018v10i10.27376.
34. Duru, C. E., Duru, I. A., Ikpa, C. B. C., & Ibe, F. C. (2014). Chemical and spectra studies of the alleged killer seed of Berlinia grandiflora. IOSR. J. Appl. Chem., 7(1), 14-18. https://doi.org/10.9790/5736-07121418.
35. Olatunji, K. T., Oladosu, P. O., & Kolawole, M. O. (2025). In vitro antimycobacterial potential, acute toxicity and GC-MS analysis of Berlinia grandiflora (Vahl) Hutch. & Dalziel and Senna occidentalis (L.) link leaves extracts. Pharmacological Research - Natural Products, 6, 100154. https://doi.org/10.1016/j.prenap.2025.100154.
36. Baptista, R., Bhowmick, S., Shen, J., & Mur, L. A. J. (2021). Molecular docking suggests the targets of anti-mycobacterial natural products. Molecules, 26(2), 475. https://doi.org/10.3390/molecules26020475.
37. Ribeiro, J. A., Hammer, A., Libreros-Zúñiga, G. A., Chavez-Pacheco, S. M., Tyrakis, P., de Oliveira, G. S., Kirkman, T., El Bakali, J., Rocco, S. A., Sforça, M. L., Parise-Filho, R., Coyne, A. G., Blundell, T. L., Abell, C., & Dias, M. V. B. (2020). Using a Fragment-Based Approach to Identify Alternative Chemical Scaffolds Targeting Dihydrofolate Reductase from Mycobacterium tuberculosis. ACS. Infect. Dis., 6, 2192-2201. https://dx.doi.org/10.1021/acsinfecdis.0c00263.
38. Manjunatha, U. H., Rao, S. P. S., Kondreddi, R. R., Noble, C. G., Camacho, L. R., Tan, B. H., Ng, S. H., Ng, P. S., Ma, N. L., & Lakshminarayana, S. B. (2015). Direct Inhibitors of InhA Active against Mycobacterium tuberculosis. Sci. Transl. Med., 7(269), 269ra3. https://dx.doi.org/10.1126/scitranslmed.3010597.
39. Malikyan, S., & Olson, A. J. (2015). Small-Molecule Library Screening by Docking with PyRx. Methods Mol. Biol., 1263, 243-250. https://doi.org/10.1007/978-1-4939-2269-7-19.
40. Trott, O., & Olson, A. J. (2010). AutoDock Vina: Improving the speed and accuracy of docking with a new scoring function, efficient optimization, and multithreading. J. Comput. Chem., 31(2), 455–461. https://doi.org/10.1002/jcc.21334.
41. Hsu, K. C., Chen, Y. F., Lin, S. R., & Yang, J. M. (2011). iGEMDOCK: a graphical environment of enhancing GEMDOCK using pharmacological interactions and post-screening analysis. BMC Bioinformatics,12(1), S33. https://doi.org/10.1186/1471-2105-12-S1-S33.
42. DeLano, W. L. (2002). Pymol: An open-source molecular graphics tool. CCP4 Newsl. Protein Crystallography, 40(1), 82–92.
43. Xu, L., Jiang, W., Jia, H., Zheng, L., Xing, J., Liu, A., & Du, G. (2020). Discovery of Multitarget Directed Ligands Against Influenza A Virus from Compound Yizhihao Through a Predictive System for Compound-Protein Interactions. Frontiers in Cellular and Infection Microbiology, 10, 16. https://doi.org/10.3389/fcimb.2020.00016.
44. Kannan, R., Alharbi, N. S., Kadaikunnan, S., Rajaram, S. K., & Alexander, R. A. (2016). In silico Analysis of Phytoconstituents from Allium sativum as Potential Inhibitors of Inha in Mycobacterium tuberculosis. Brazilian Archives of Biology and Technology, 59, 16160109. https://doi.org/10.1590/1678-4324-2016160109.
45. Argyrou, A., Vetting, M. W., Aladegbami, B., & Blanchard, J. S. (2006). Mycobacterium tuberculosis dihydrofolate reductase is a target for isoniazid. Nature structural & molecular biology, 13(5), 408–413. https://doi.org/10.1038/nsmb1089.
46. Endriyatno, N. C. (2022). Molecular Docking of Betel Leaf (Piper betle L.) on Protein Dihydrofolate reductase of Mycobacterium tuberculosis. Science and Community Pharmacy Journal, 1(1), 1-5.
47. Khan, T., Dixit, S., Ahmad, R., Raza, S., Azad, I., Joshi, S., & Khan, A. R. (2017). Molecular docking, PASS analysis, bioactivity score prediction, synthesis, characterization and biological activity evaluation of a functionalized 2-butanone thiosemicarbazone ligand and its complexes. J. Chem. Biol., 10(3), 91–104. https://doi.org/10.1007/s12154-017-0167-y.